University of Groningen

Physics Bachelor Thesis

Dynamics of Levitated Nanospheres in a Modulated Potential

Authors:
Manal Alsairafi *(s3548945)*

First Examiner:
Steven Hoekstra
Second Examiner:
Anastasia Borschevsky

Abstract

In this research, the trapping of dielectric silica nanospheres in a modulated potential is explored in the underdamped regime. The particle is trapped via the method of optical tweezers in which a focused gaussian laser beam of wavelength much higher than the nanosphere's diameter is used. The field of the beam induces a dipole moment in the particle thus attratcing it to its gradient thereby trapping it. In order to study the particle's dynamics in the underdamped regime, the optical trap in the setup operates in a vacuum chamber, such that the pressure is decreased, decreasing the damping rate to be much lower than the oscillation frequency of the particle. The trapping potential is modulated through modulating the beam intensities by utilizing an electro-optic modulator (EOM), which is coupled to a function generator, such that a square wave function is generated, allowing us to observe the particle's reactions to sudden changes in the potential. The results of the study focus on analysing the power spectral density of the oscillations, the position distribution of the particle and its evolution with time upon modulating the trap's intensity. Studies focused on optical trapping of nanoparticles, in the underdamped regimes allow for the development of the fields of quantum optics and the mechanics of mesoscopic objects.

Dynamics of Levitated Nanospheres in a Modulated Potential

July 20, 2021

Contents

1 Introduction

Well after the development of the theory of electromagnetism, it was discovered that photons carry momentum, this means that light is able to exert forces onto massive objects. It was also discovered that massive objects have the property of polarizability, meaning they can acquire an electric dipole moment. This means that a dielectic sphere in a laser beam tends to move towards the center, this was realised in 1970 by Arthur Ashkin. Ashkin took this phenomena a step furthur, such that when the laser beam is highly focused, the sphere would be trapped, forming what is called an optical tweezer [1]. Later in 2018, Arthur Ashkin was awarded the Nobel prize in physics for this discovery.

These optical traps or tweezers have many applications beyond purely studying the physical phenomena, of which are applications in biology, such that the mechanical properties of organisms and biological systems can be studied. Optical tweezers are also applied in engineering, where microscopic heat engines can be built based on the theories of optical trapping [11] .

1.1 Motivation

With the various applications of optical tweezers, the study of optical trapping has been of high interest. Optical trapping in the overdamped regime has been more theoretically established, as it is more accessible in applications, in this research we go in the other direction. Optical trapping in underdamped regimes using nano-scaled particles allow us to explore the quantum effects of the phenomena [4], research around optical tweezers in such conditions are currently limited, thus we focus the study to it in attempts of contributing to the field.

1.2 Goal and research questions

The aim of the project is to study nanosphere dynamics in a modulated potential within the underdamped regime. This is done by setting up an optical tweezer to trap a silica nanosphere of diameter 143 nm. The optical trap is modulated such that the particle experiences a sudden (step) change in the intensity of the trap. The trap is set up in a vacuum chamber such that the pressure can be controlled, and underdamped motion is achieved. Differential detection methods are used to detect the oscillations of the trapped particle in terms of fluctuations in the detected signals. In order to realise the dynamics of the nanosphere we calibrate the signals to find the displacement of the particle. Two methods of calibration are preformed and compared.

With the goal in mind, the following research questions are explored in the study:

- How do the different calibration methods compare with one another quantitatively?
- How do the properties of the particle's motion change when modulating the beam's intensity, and how does the particle transition and settle with the changes?

2 Theory

Optical tweezers work on the principles of polarizability of materials, such that the trapped particle gains a dipole moment along the electric field of the optical trap [1].

The optical trap in this study operates in a vacuum chamber where the pressure is decreased to be as low as ~ 10 mbar, thus, besides the optical effects of the electromagnetic field on the trapped particle, the effects of the Brownian motion of the particles in the surrounding gas, as well as the temperature of the gas have taken into account.

In this section, the theory behind optical tweezers is discussed, which involves studying the electromagnetic field of the trap's beam and the dominant forces acting on the particle due to the optical setup. The particle's behaviour in such setup within the underdamped regime, as well as the implications of modulating the laser properties are theoretically analysed.

2.1 Optical tweezers

2.1.1 The Gaussian beam

Laser beams usually have a Gaussian beam profile (figure 2.1), to use the laser in an optical tweezer, it is focused via a microscope objective with a certain numerical aperture NA. The numerical aperture defines the range of angles that the objective can accept or emit light at. It is expressed as

$$\mathrm{NA} = n_m \sin\theta_{max} \tag{2.1}$$

where n_m is the refractive index of the medium in which the lens (the microscope objective) operates. θ_{max} defines the maximum half-angle of the light cone exiting the focus of the beam. The electric field of the light as depicted in figure 2.1 is found by using the paraxial approximation ($\sin\theta = \theta$) and integrating a Gaussian electric field over the phase space as to account for the interference of the plane waves [9]

$$\mathbf{E}(\rho, z) = E_0 \frac{w_0}{w(z)} e^{-\frac{\rho^2}{w(z)^2} + \mathbf{i}\phi(\rho,\mathbf{z})} \hat{\mathbf{n}} \tag{2.2}$$

with $E_0\hat{\mathbf{n}}$ the constant field vector in the x, y plane, w_0 the beam waist, z_0 the Rayleigh range which indicates the distance from the center to the point where the beam radius increases by $\sqrt{2}$, it is dependent on the wavelength of the laser λ and the beam waist, given by $z_0 = \pi w_0^2/\lambda$. These parameters are illustrated in figure 2.1, and $\rho^2 = x^2 + y^2$, the following is also defined

$$w(z) = w_0\sqrt{(1 + z^2/z_0^2)} \qquad \text{beam radius,} \tag{2.3a}$$

$$\phi(\rho, z) = \frac{2\pi}{\lambda} z - \eta(z) + \frac{2\pi}{\lambda}\frac{\rho^2}{2R(z)} \qquad \text{phase,} \tag{2.3b}$$

$$\eta(z) = \arctan z/z_0 \qquad \text{phase correction,} \tag{2.3c}$$

$$R(z) = z(1 + z^2/z_0^2) \qquad \text{wavefront radius.} \tag{2.3d}$$

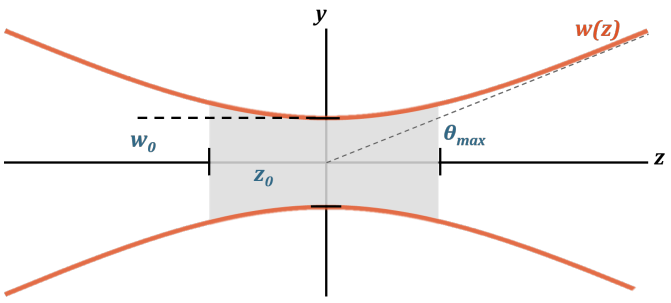

Figure 2.1: Profile of a focused Gaussian beam along the optical axis z

2.1.2 The optical forces

The nanosphere trapped in the experiment is a dielectric Silica nanosphere with diameter $d = 143 \pm 1$ nm and the trapping laser has wavelength $\lambda = 1064$ nm, thus we limit the discussion on the forces acting on the particle to the Rayleigh regime ($d \ll \lambda$) where the particle is considered a dielectric point particle [5]. The optical force in this regime is given by the sum of the gradient force $\mathbf{F}_{\text{grad}}(\mathbf{r})$ and the scattering force $\mathbf{F}_{\text{scat}}(\mathbf{r})$

$$\mathbf{F}(\mathbf{r}) = \mathbf{F}_{\text{grad}}(\mathbf{r}) + \mathbf{F}_{\text{scat}}(\mathbf{r}) \tag{2.4}$$

The gradient force is the result of the Lorentz force on the dipole induced by the field due to the polarizability of the dielectric nanosphere, defined as

$$\mathbf{F}_{\text{grad}}(\mathbf{r}) = \frac{\alpha'}{4}\nabla I_0(\mathbf{r}) \tag{2.5}$$

and the scattering force is due to the incidence of beam photons on the nanosphere, given by

$$\mathbf{F}_{\text{scat}}(\mathbf{r}) = \frac{\alpha''}{2} I_0(\mathbf{r})\nabla\phi(\mathbf{r}) \tag{2.6}$$

where $I_0(\mathbf{r}) = \mathbf{E}_0(\mathbf{r})^2$ is the field intensity, $\phi(\mathbf{r})$ is the phase as given by equation 2.3b. α' and α'' are the real and imaginary components of the effective polarizability α_{eff}. The polarizability of a spherical particle with volume V and dielectric constant ϵ_p in a medium with dielectric constant ϵ_m is given by the Clausius-Mossotti relation [2]

$$\alpha = 3V\epsilon_0 \frac{\epsilon_p - \epsilon_m}{\epsilon_p + 2\epsilon_m} \tag{2.7}$$

Momentum can be transferred from the laser photons to the particle either by scattering or absorption, which modifies the optical forces. This effect is taken into account in the effective polarizability given by

$$\alpha_{\text{eff}} = \alpha \left(1 - \mathbf{i}\left(\frac{2\pi}{\lambda}\right)^3 \frac{\alpha}{6\pi\epsilon_0}\right)^{-1} \tag{2.8}$$

From equations 2.5, 2.6 and 2.2, we can derive the forces. The final expression is arrived at after making an approximation for small displacements $|r| \ll \lambda$, we also define the wavenumber $k = 2\pi/\lambda$ [3]

$$\mathbf{F}_{\text{grad}}(\mathbf{r}) \approx -\begin{pmatrix} \kappa_x[1 - 2x^2/w_x^2 - 2y^2/w_y^2 - 2z^2/z_0^2]x \\ \kappa_y[1 - 2x^2/w_x^2 - 2y^2/w_y^2 - 2z^2/z_0^2]y \\ \kappa_z[1 - 2x^2/w_x^2 - 2y^2/w_y^2 - 2z^2/z_0^2]z \end{pmatrix} \tag{2.9}$$

$$\mathbf{F}_{\text{scat}}(\mathbf{r}) \approx \frac{\alpha''}{\alpha'}\kappa_z \begin{pmatrix} kxy \\ kyz \\ \gamma_0 + (2 - kz_0)z^2/z_0 + [k/2 + 2\gamma_0/w_x^2]x^2 + [k/2 + 2\gamma_0/w_y^2]y^2 \end{pmatrix} \tag{2.10}$$

with $\gamma_0 = (kz_0^2 - z_0)$, w_i the beam width, and κ_i the trap stiffness in the three dimensions with $i = x, y, z$. The stiffness is defined as follows

$$\kappa_x = \alpha' E_0^2/w_x^2 \tag{2.11a}$$

$$\kappa_y = \alpha' E_0^2/w_y^2 \tag{2.11b}$$

$$\kappa_z = \alpha' E_0^2/2z_0^2 \tag{2.11c}$$

From equation 2.9 it can be seen that the gradient force represents a restoring elastic force $F = -\kappa x_i$ analogous to Hooke's law with κ the trap's stiffness.

2.1.3 The optical potential

In the Rayleigh regime, the scattering force can be negligible, and the potential of the trap is defined in terms of the conservative gradient force

$$\mathbf{F}_{\text{tot}}(x_i) \approx \mathbf{F}_{\text{grad}}(x_i) \approx -\kappa x_i \tag{2.12}$$

we can thus find the potential of the optical trap

$$\begin{aligned} U(x_i) &= -\int F(x_i)dx \\ &= \frac{1}{2}\kappa x_i^2 \end{aligned} \tag{2.13}$$

This represents a harmonic potential in which the trapped particle oscillates [10]. A particle's position in a potential within a thermal bath follows the Boltzmann distribution

$$P(x_i) = \exp(-U(x_i)/k_B T) \tag{2.14}$$

where $k_B T$ is the mean energy of the thermal bath. Given the potential in equation 2.13, we find that the position distribution is Gaussian

$$P(x_i) = \exp(-\kappa x_i^2/2k_B T) \tag{2.15}$$

2.2 The particle's behaviour in the trap

The particle, with mass m and radius a, undergoes optical forces induced by the laser as well as Brownian motion. With a harmonic potential, the particle in the trap behaves like a harmonic oscillator. Since the study focuses on trapping the particle in low pressures around 10 mbar, we expect that the damping rate is much smaller than the frequency of the oscillations, thus the equation of motion is given by the equation of motion of a harmonic oscillator in the underdamped regime

$$\ddot{x}_i(t) + \Gamma_0 \dot{x}_i(t) + \omega_{0,i}^2 x_i(t) = \frac{1}{m}[F_{\text{fluc}}(t) + F_{\text{opt}}(t)] \tag{2.16}$$

here, ω_0 is the angular frequency of the particle, and it is defined in terms of the trap's stiffness and the particle's mass

$$\omega_{0,i} = \sqrt{\frac{\kappa_i}{m}}, \tag{2.17}$$

Γ_0 is the damping rate, which is the result of particle collision with the gas molecules of the heat bath. This is given by

$$\frac{\Gamma_0}{2\pi} = 3\mu_v \frac{a}{m} \frac{0.619}{0.619 + K_n}(1 + c_K) \tag{2.18}$$

with $c_K = 0.31K_n/(0.785 + 1.152K_n + K_n^2)$, where $K_n = \bar{l}/a$ is the Knudsen number, $\bar{l}$ is the mean free path given by

$$\bar{l} = \frac{k_B T}{\sqrt{2}\pi d_m^2 p} \tag{2.19}$$

and μ_v is the viscosity coeffecient given by

$$\mu_v = \frac{2\sqrt{m_{gas} k_B T}}{3\pi^{3/2} d_m^2} \tag{2.20}$$

where d_m is the diameter of the gas molecules, m_{gass} is their mass and p the pressure of the gas. [8]
The forces acting on the particle are given by the optical forces of the Gaussian beam $F_{\text{opt}}(t)$ (eq. 2.4) and the fluctuation forces $F_{\text{fluc}}(t)$ which describe the Brownian motion. The fluctuation forces are described by the random Langevin force satisfying [12]

$$\langle F_{\text{fluc}}(t) F_{\text{fluc}}(t') \rangle = 2m\Gamma_0 k_B T \delta(t - t') \tag{2.21}$$

2.3 Potential modulation

The research aims to study the particle's behaviour after experiencing a modulation in the trapping potential. The change is induced by changing the laser intensity, proportional to E_0^2, thereby changing the trap's stiffness. The change will in turn change the frequency of the oscillation (eq. 2.17) as well as the position distribution of the particle in the trap (eq. 2.15). The changes when going from a low trap stiffness to a higher stiffness are illustrated in figure 2.2. [7]

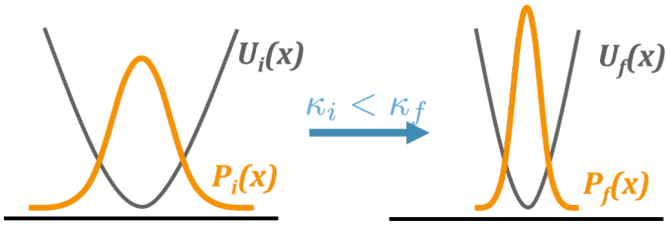

Figure 2.2: modulation of the trap's stiffness and effect on the particle's position distribution in the trap

2.3.1 Particle relaxation

Upon changing the trap's stiffness, the particle transitions from an initial equilibrium state characterised by the stiffness before the change κ_i to a final equilibrium state characterised by the final stiffness κ_f. The time it takes for the particle to settle to the final state is the relaxation time τ_{relax} defined as [8]

$$\tau_{\text{relax}} = \frac{2\pi}{\Gamma_0} \tag{2.22}$$

This indicates that at lower pressures (lower damping rates) when the interactions with the heat bath's particles are lowered, the particle takes more to transition between the two states.

3 Methods

The research aims to study the particle's behaviour in an optical tweezer in the underdamped regime, thus, the experiment is setup such that the trap operates in a vacuum chamber. Here, the different components of the experimental setup are explained as well as the data collection and calibration methods.

3.1 Experimental setup

3.1.1 Overview of the setup and its components

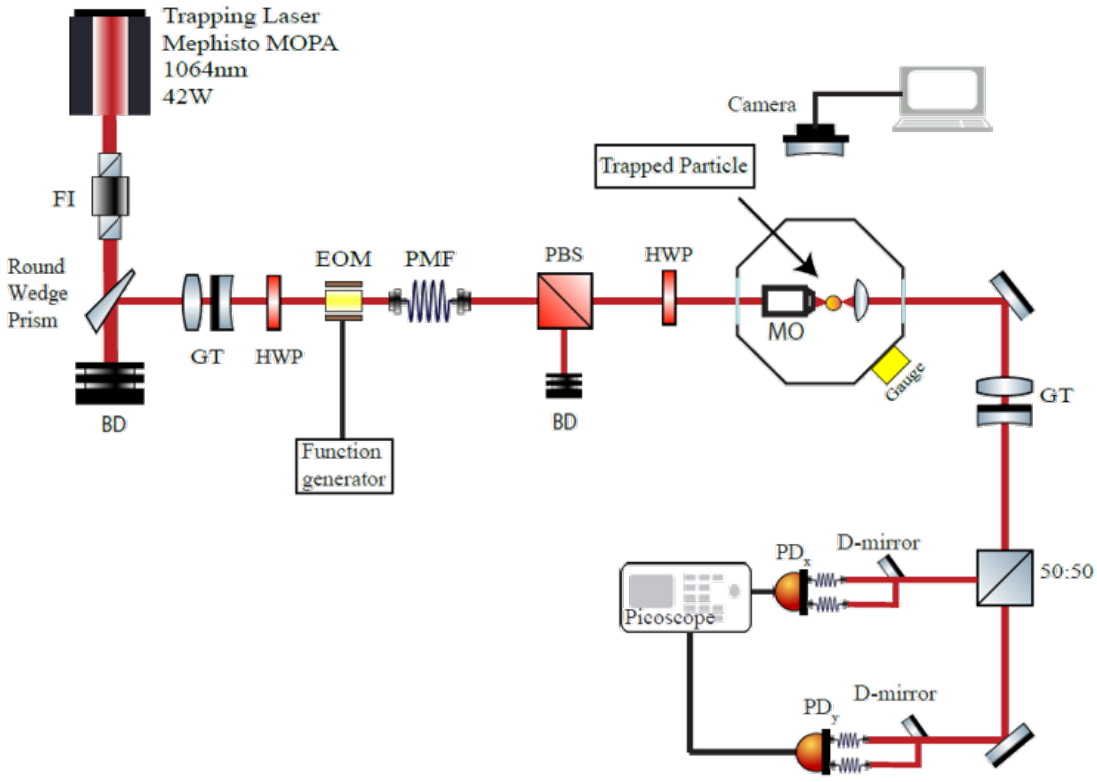

Figure 3.1: Schematic of the optical trap setup.

The experiment is set such that it consists of these main components: The trapping laser, the electro-optic modulator, the vacuum chamber and the detection system, the schematic of this is shown in figure 3.1. Below, these components are dissected and explained following the path of the beam, starting at the laser source:

(1) **Trapping laser**
The Mephisto MOPA laser with wavelength 1064 nm is used, it produces a Gaussian profile in the transverse electromagnetic mode (TEM00) [6]. The laser source is supplied with a current of 54 A. The laser beam goes through a Farady Isolator (FI) to prevent back reflection, it is then steered towards the direction of the electro-optic modulator (EOM) using a round wedge prism. The directed beam then travels through a Galilean type beam expander (GT), which consists of a concave lens and a bi-convex lens spread some distance apart to fix the beam diameter appropriately to go through the rest of the optical setup. The light travels through a half-wave plate (HWP) before continuing.

(2) **Electro-optic modulator**
In order to apply modulations to the trap's stiffness, an electro-optic modulator (EOM) is used. The EOM is connected to a function generator via which a square wave with a set amplitude A_{mod} and frequency f_{mod} is applied as to study the nanosphere's response to sudden changes.

(3) **The vacuum chamber**
Before going to the vacuum chamber, the modulated beam travels through a polarization-maintaining optical fiber (PMF). The PMF is used because the trapping laser and the EOM are separated from the vacuum chamber and detection system, thus, the beam is directed towards the vacuum chamber without altering its polarization. The beam then goes through a polarizing beam splitter (PBS) such that the transmitted beam component is p-polarized, the reflected component (s-polarized) is discarded in a beam dump (BD). The light goes through another half-wave plate, then to the vacuum chamber.

The trap is set up in the vacuum chamber, a microscope objective (MO) with numerical aperture $NA = 0.8$ is used to focus the beam forming the optical trap. The beam is then collimated using an aspheric lens before exiting the vacuum chamber.

A similar setup using an MO with the same numerical aperture and a laser beam with the same wavelength determines experimentally that the resulting beam widths are $w_x = 687$ nm and $w_y = 542$ nm [3].

(4) **Detection system**
The detection system consists of a CCD camera placed outside the vacuum chamber. It does not give an indication of the trapped nanosphere's size due to the scattering of light on the particle. The camera is connected to the LabView program showing the trap. Figure 3.2 shows snapshots from the camera.

After travelling through the vacuum chamber, the beam is directed with a mirror and its diameter is adjusted with a Galilean type beam expander (GT) to be detected. The light then goes through a 50:50 beam splitter to split the horizontal (x) and vertical (y) directions, the signals along the optical axis (z) are not detected. The method of differential detection is used in the experiment as to reduce noise. This method requires splitting the different orientations equally using D-mirrors: the horizontal signal is split into right and left components, and the vertical signal into top and bottom. These signals are then detected using photodiodes (PD), the difference between the split components of each orientation is measured and sent to an oscilloscope (PicoScope) where the final signals are registered. The signal of the EOM is also registered in the oscilloscope.

3.1.2 Particle loading

The nanospheres used in the experiment are dielectric silica particles with a diameter of 143 nm and density 1.85 g/cm^3. To load the particles into the vacuum chamber, a medical nebuliser, which vaporises the liquids put in it, is used. The silica nanospheres come together in liquid form, and for it to be vapourised into the vacuum chamber a solution of the particles with ethanol is prepared. 50 mg of the silica particles is mixed with 1 ml of ethanol and put in an ultrasonic bath, this ensures that the particles do not clump together.

After the solution is prepared and put in the nebuliser, it is vaporised into the vacuum chamber through a funnel connected to the opening of the chamber. The nebulising process is depicted in figure 3.2. When the particle solution is loaded, the vacuum chamber is closed. After ensuring the particle is trapped, the valve of the vacuum chamber is open such that air is released and the pressure is decreased. The pressure is read via a gauge connected to the chamber. This part of the setup is most delicate and any harsh movement causes the particle to be lost from the trap, thus closing the chamber should be done carefully, and opening the chamber's valve should be done slowly.

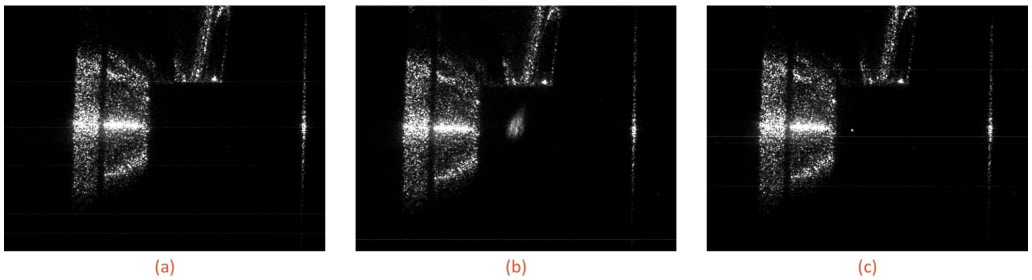

Figure 3.2: Snapshots from LabView: **(a)** The vacuum chamber without a trapped particle, on the left is the MO, on the right is the aspheric lens and on the top the loading funnel. **(b)** The vacuum chamber after nebulising, the 'blob' shows the flow of particles. **(c)** The vacuum chamber with a trapped particle represented by the small dot close to the MO.

3.2 Data acquisition and calibration

3.2.1 The raw signals and modulation

As mentioned in the experimental setup, the modulation in the optical potential is done via an electro-optic modulator coupled with a function generator. To collect a large enough statistical sample, the modulation is set as a square wave, where the data over one period then represent the particle's oscillations in a potential with a sudden change of stiffness that occurs at half the period. In order to study the particle's displacement, the following steps are preformed:

1. The horizontal and vertical signals as well as the modulation signal are saved with a sampling rate of 1×10^6 s^{-1} for a sampling time of 10 seconds.

2. Due to background noise, low frequency oscillations (< 100 Hz) occur in the signal, and because of the finite range of the detection system, the signals tend to saturate at some points. The saturated signals are removed from the data set.

3. Since the laser's intensity is being modulated, the intensity of the signal itself changes, thus the amplitude of the signal's oscillations does not become reflective of the displacement of the particle in the trap. Thus, the signals in both the horizontal and vertical directions are separated into signals corresponding to the high intensities of the modulated potential and those corresponding to the lower intensities.

4. The low frequencies are filtered, this is done by subtracting the mean value of the data points over half a period (when the intensity is of the beam is constant) from the data points. This is applied on all half periods of the data set after excluding the saturated signals. The reason this is done instead of a butterworth filter is to avoid neglecting the effects of the damping on the particle.

5. The power spectral densities of the oscillations in either direction and corresponding to the higher and lower laser beam intensities are plotted to find the frequency of oscillation of the particle.

6. The filtered signals are theoretically calibrated to find the displacement of the particle in meters. This can be done via two methods discussed in the following sections.

Steps 3-5 are preformed via a python program, see appendix A.

3.2.2 Calibration via position distributions

Given the linear trapping potential $U(x) = kx^2/2$ (eq. 2.13), and that the particle's position distribution follows a Boltzmann distribution, we find the expected distribution to be

$$P_x = \exp\left(-kx^2/2k_BT\right) \tag{3.1}$$

with k the trap's stiffness, k_B Boltzmann's constant and T the absolute temperature. This follows a normal distribution with variance $\sigma_x^2 = k_B T/k$. The trap's stiffness can be calculated directly using the Power Spectral Density plots where the power peaks at the oscillation frequency of the particle f_0 given in Hz. Using the relation between the angular frequency of the particle and the trap's stiffness (eq. 2.17), we find that

$$k = m \cdot (2\pi f_0)^2 \tag{3.2}$$

The temperature T is given by the temperature of the heat bath, i.e. the temperature in vacuum chamber, this is taken as room temperature (293 K).
To get to the displacement in meters, we assume linear calibration with a constant $b_{V\to x}$:

$$x[\mathrm{m}] = b_{V\to x} V[\mathrm{V}] \tag{3.3}$$

This assumption also means that the frequency of the oscillations in the signal in Volts is equal to the frequency of the oscillations in the particle's displacement in meters.
The distribution of signal oscillations then becomes

$$P_V = \exp\left(-k b_{V\to x}^2 V^2 / 2 k_B T\right) \tag{3.4}$$

with variance $\sigma_V^2 = k_B T/k b_{V\to x}^2$. By fitting the distribution obtained experimentally to a Gaussian distribution, finding the oscillation frequency, and using equation 3.2, we find the calibration constant to be

$$b_{V\to x} = \sqrt{\frac{1}{\sigma_V^2}\left(\frac{k_B T}{k}\right)} \tag{3.5}$$

The python code used to calibrate the data with this method is in appendix B.

3.2.3 Calibration via power spectral densities

This method is adopted from Jamie Vovrosh's PhD thesis [13]. The expected power spectral density (PSD) follows a Lorenzian profile given by

$$S_{xx}[\mathrm{m}^2/\mathrm{Hz}](\omega) = \frac{k_b T}{\pi m}\frac{\Gamma_0}{(\omega_0^2 - \omega^2)^2 + \omega^2\Gamma_0^2} \tag{3.6}$$

This equation follows from the particle's displacement in meters, since the calibration at constant beam intensity is linear, a constant γ with units of V/m is included to find the PSD in terms of voltage

$$S_{xx}[\mathrm{V}^2/\mathrm{Hz}](\omega) = \gamma^2\frac{k_b T}{\pi m}\frac{\Gamma_0}{(\omega_0^2 - \omega^2)^2 + \omega^2\Gamma_0^2} \tag{3.7}$$

Equation 3.7 is used to fit the PSDs generated (step 5). Similar to the previous method, T is taken to be the temperature in the vacuum chamber approximated to be room temperature. From the fit, we find the damping rate Γ_0, from which the pressure can be found, the oscillation frequency ω_0 and the constant γ from which we find the calibration constant

$$b_{V\to x} = \frac{1}{\gamma} \tag{3.8}$$

Through this method, we also calculate the relaxation time by taking the inverse of the damping rate (eq. 2.22). The python code for this process is in appendix C. Note that the program is written such that the PSD is given as a function the frequency rather than the angular frequency, so the parameters found are $f_0 = \omega_0/2\pi$ and $\Gamma_0/2\pi$.

4 Results and discussions

To explore the dynamics of our silica nanospheres in the optical trap, four data sets have been collected by applying the square wave modulation to the laser beam, first with an amplitude of 5V and a frequency of 1 kHz, data with this modulation have been collected at different pressures: 30 mbar, 20 mbar and 10 mbar. Second, after achieving the lower pressure, the beam is modulated with an amplitude of 0.5V and 0.1 kHz. The process as explained in the methods is then applied.

4.1 The collected data

Below in figures 4.1, 4.2, 4.3 and 4.4 the full set of collected raw data are depicted as well as a zoom in of the data taken over one period.

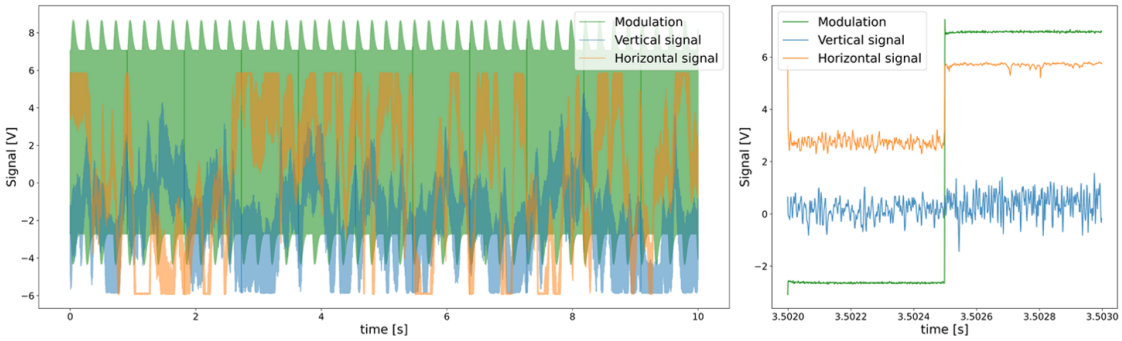

Figure 4.1: **Data Set A** - vertical and horizontal trap signals in response to a modulated signal: square wave with 5V amplitude and 1 kHz frequency, at pressure 30 ± 1 mbar. On the right: the signals over one period of modulation.

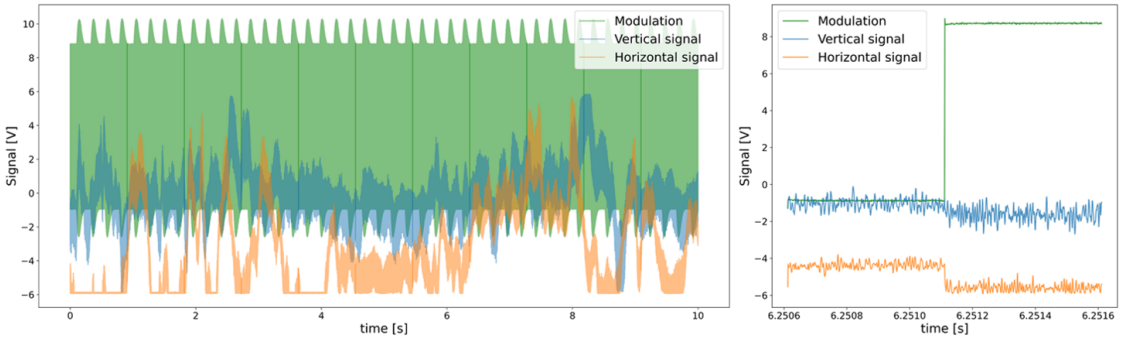

Figure 4.2: **Data Set B** - vertical and horizontal trap signals in response to a modulated signal: square wave with 5V amplitude and 1 kHz frequency, at pressure 20 ± 1 mbar. On the right: the signals over one period of modulation.

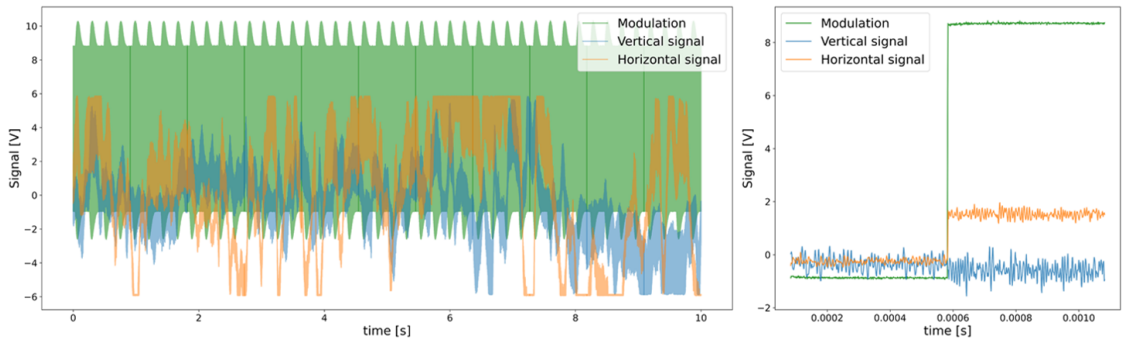

Figure 4.3: **Data Set C** - vertical and horizontal trap signals in response to a modulated signal: square wave with 5V amplitude and 1 kHz frequency, at pressure 10 ± 1 mbar. On the right: the signals over one period of modulation.

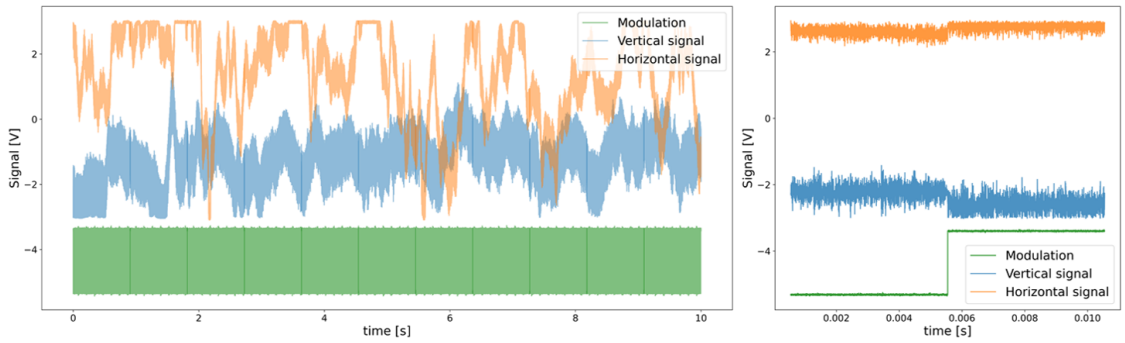

Figure 4.4: **Data Set D** - vertical and horizontal trap signals in response to a modulated signal: square wave with 0.5V amplitude and 0.1 kHz frequency, at pressure 9 ± 1 mbar. On the right: the signals over one period of modulation.

It can be seen that the signal saturates and goes beyond the range of the oscilloscope for all data sets. It should also be noted that the horizontal signals are less stable than than the vertical, this is due to errors and the imprecision in the optical setup as a result of manually splitting the beams at the D-mirrors. The noise can be reduced in future setups by decreasing the beam path by shortening the distances between the optical components.

4.2 Power spectral density analysis

Below the power spectral densities are graphed, and using equation 3.7 with the code in appendix C, the fits are found. Figures 4.5, 4.6, 4.7 and 4.8 show the PSDs corresponding to the different orientations at the different intensities and pressures as well as the fitting parameters. The pressures are found from the gauge attached to the vacuum chamber, using the damping rate averaged over the different signals (horizontal and vertical at higher and lower intensities) along with equations 2.18, 2.19 and 2.20 the pressure can be calculated and compared to the readings on the gauge. It should be noted that the gauge's accuracy and precision are not high. The diameter and mass of gas molecules are taken as those of air molecules: $d_m = 0.372$ nm and $M_{gas} = 28.97 \times 10^{-3}$ kg/mol [8].

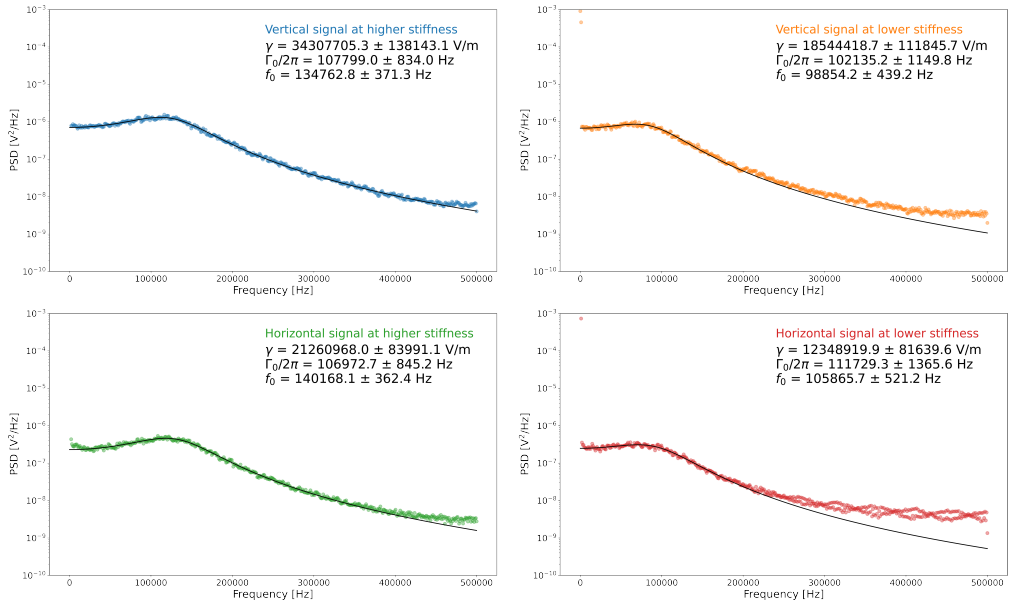

Figure 4.5: The PSDs and fits of signals collected with 10V modulation at 30 ± 1 mbar. The pressure found from the fitting is $p_{fit} = 18.7 \pm 4.0$ mbar.

It is observed that at 30 mbar (fig. 4.5), that the particle oscillates in the critical damping regime where $\Gamma \sim \omega_0$, and that the PSD peak is wide.

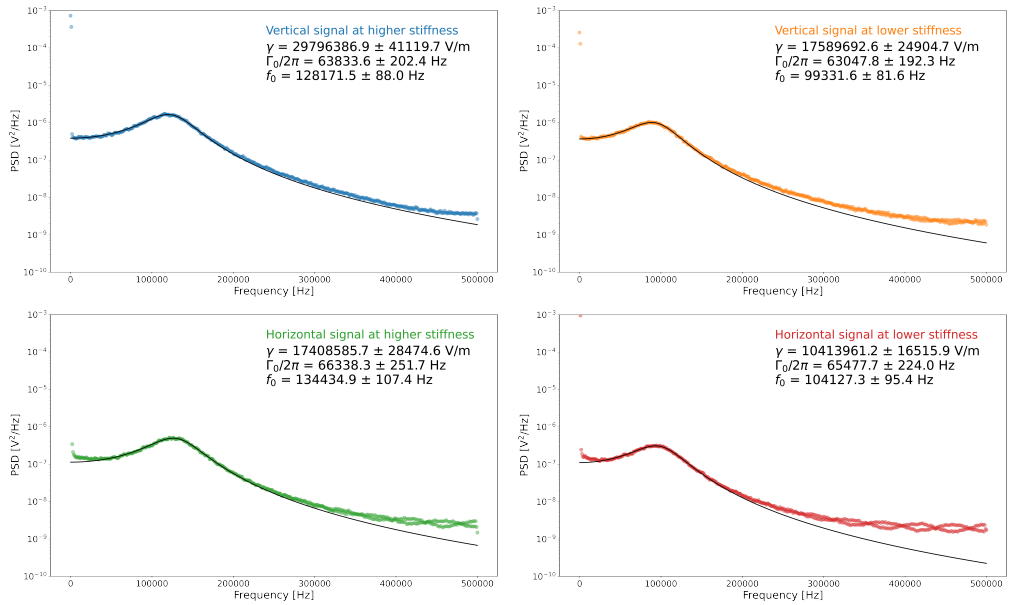

Figure 4.6: The PSDs and fits of signals collected with 10V modulation at 20 ± 1 mbar. The pressure found from the fitting is $p_{fit} = 11.2 \pm 1.5$ mbar.

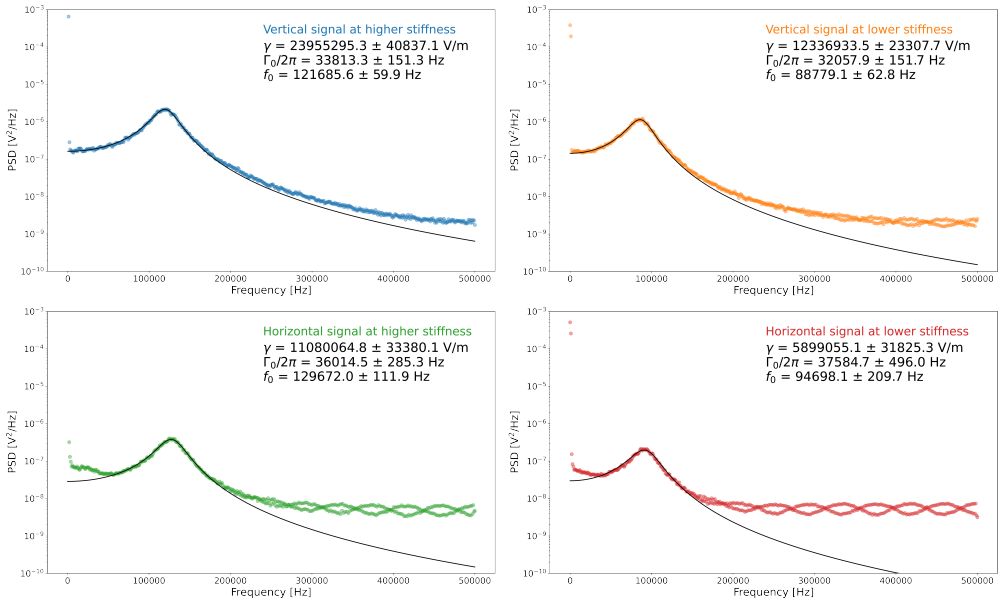

Figure 4.7: The PSDs and fits of signals collected with 5V modulation amplitude at 10 ± 1 mbar. The pressure found from the fitting is $p_{fit} = 6.0 \pm 0.5$ mbar.

As the pressure is decreased, the damping rate decreases and the width of the PSD peak narrows down, this is observed by comparing figures 4.5, 4.6 and 4.7 where the modulation applied is constant but the pressures decrease. At the lower pressure achieved, the particle oscillates at the underdamped regime where the damping rate is much lower than the oscillation frequency.

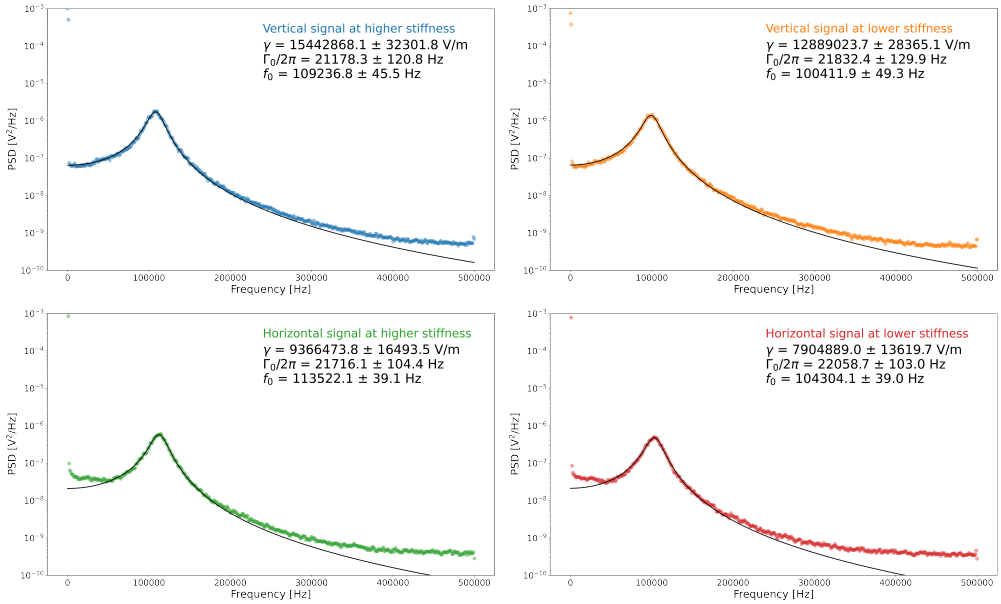

Figure 4.8: The PSDs and fits of signals collected with 10V modulation at 9 ± 1 mbar. The pressure found from the fitting is $p_{fit} = 3.8 \pm 0.2$ mbar.

By comparing the PSDs at the lower pressures (10 mbar and 9 mabr) with different modulation amplitudes applied, it can be seen that when a higher modulation is applied, such that the difference between the higher and lower beam intensities is larger, the difference between the oscillation frequencies

is greater. However, it is still seen that at the lower intensity the oscillation frequency is lower than at the higher intensity. This is in line with equations 2.11a, 2.11b, a theoretical estimation of the stiffness using these equations is difficult to make, as the beam's field strength, given the setup used, cannot be determined. It should also be noted that given the setup and the modulation, the particle escapes the optical trap when going to lower pressures.

4.3 Position distribution analysis

After fitting the PSDs, we are able to calibrate the signals using the methods described in section 3. The results of these methods at the different data sets are compared.

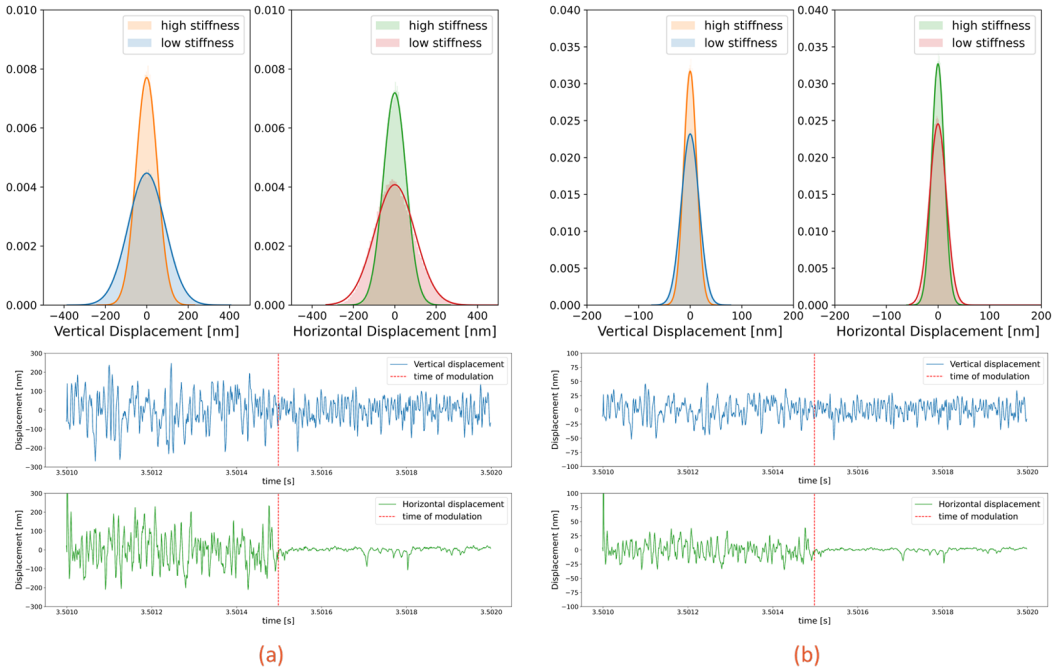

Figure 4.9: The position distributions and the displacement over one period of modulation with with 5V amplitude at 30 ± 1 mbar. **(a)** Calibrated via position distributions, **(b)** calibrated via PSDs.

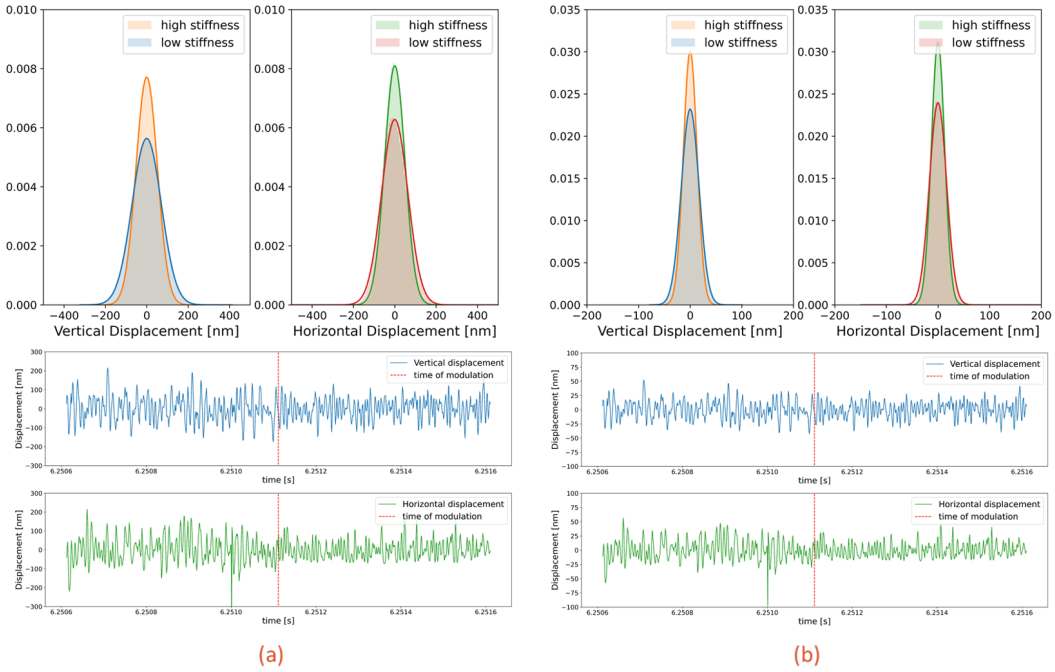

Figure 4.10: The position distributions and the displacement over one period of modulation with with 5V amplitude at 20 ± 1 mbar. **(a)** Calibrated via position distributions, **(b)** calibrated via PSDs.

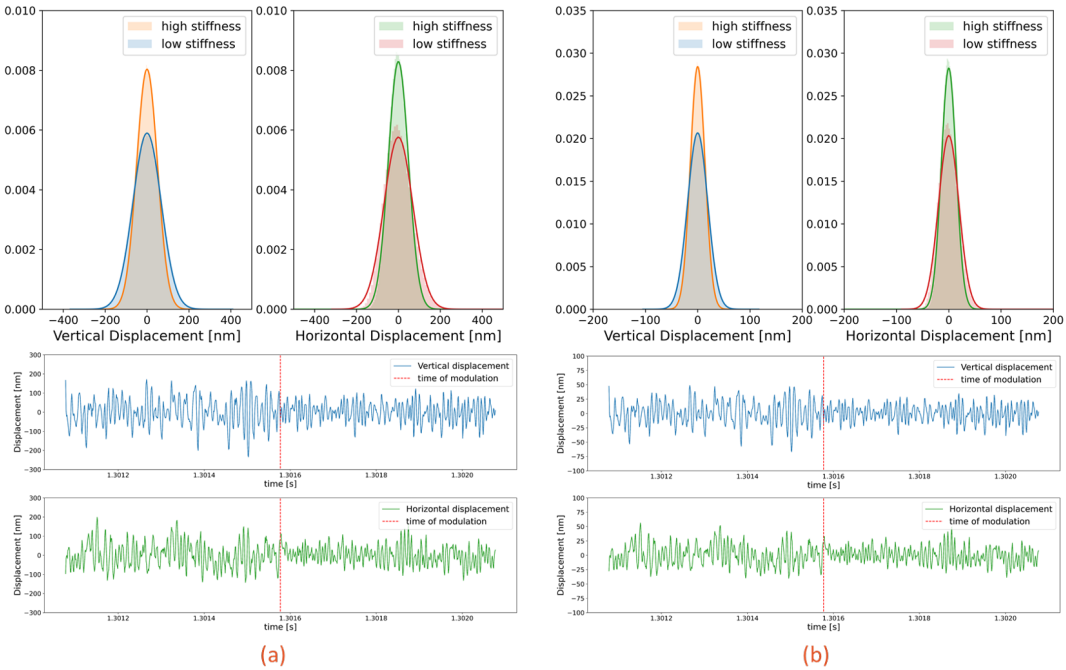

Figure 4.11: The position distributions and the displacement over one period of modulation with with 5V amplitude at 10 ± 1 mbar. **(a)** Calibrated via position distributions, **(b)** calibrated via PSDs.

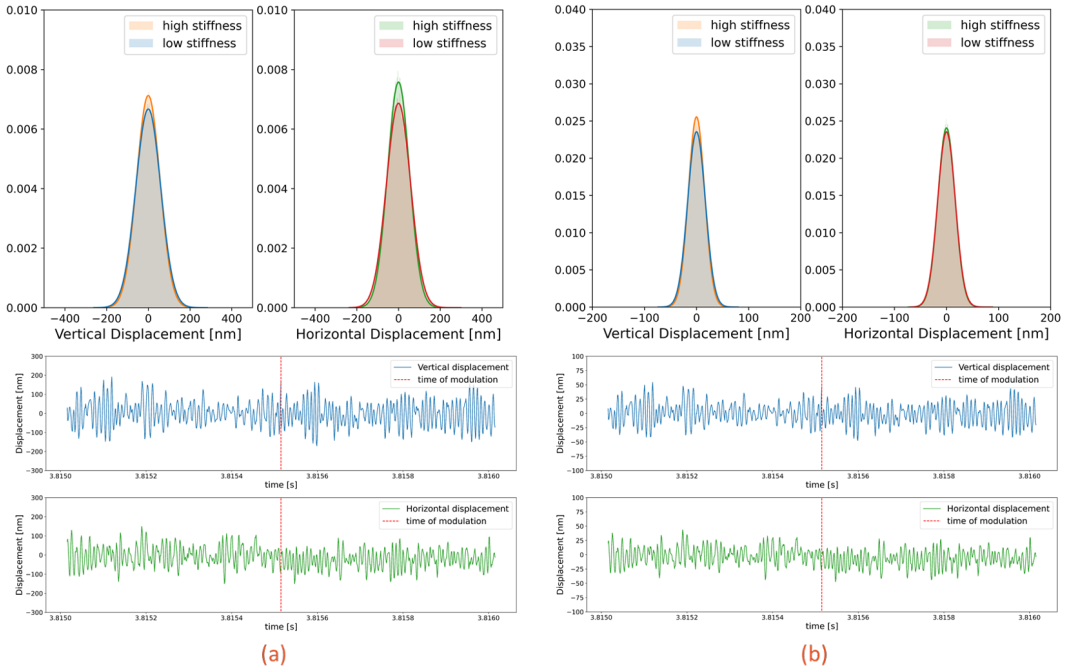

Figure 4.12: The position distributions and the displacement over one period of modulation with with 0.5V amplitude at 9 ± 1 mbar. **(a)** Calibrated via position distributions, **(b)** calibrated via PSDs.

The trends seen are in line with the theory, such that the width of the distributions are wider at the lower intensities than they are at higher intensities. And similar to the frequency peak in the PSDs, when the beam is modulated with an amplitude of 0.5 V, the difference between the widths at the higher intensity and at the lower intensity is smaller compared to when the intensity is modulated with an amplitude of 5 V. The ratios between the stiffness as calculated using equation 3.2 as well as the ratios between the widths at the higher and lower intensities are found in tables 1 and 2 below.

The Data Set	$\kappa_{x,high}/\kappa_{x,low}$	$\sigma_{x,high}/\sigma_{x,low}$ 1	$\sigma_{x,high}/\sigma_{x,low}$ 2
A	1.753 ± 0.020	0.568 ± 0.002	0.752 ± 0.004
B	1.667 ± 0.005	0.776 ± 0.003	0.770 ± 0.002
C	1.875 ± 0.002	0.695 ± 0.002	0.720 ± 0.003
D	1.185 ± 0.002	0.906 ± 0.002	0.978 ± 0.003

Table 1: The ratios of the stiffnesses and position widths at the different beam intensities in the horizontal direction. Data sets: (**A**) $A_{mod} = 5$V, $f_{mod} = 1$ kHz, $p = 30 \pm 1$ mbar (**B**) $A_{mod} = 5$V, $f_{mod} = 1$ kHz, $p = 20 \pm 1$ mbar, (**C**) $A_{mod} = 5$V, $f_{mod} = 1$ kHz, $p = 10 \pm 1$ mbar, (**D**) $A_{mod} = 5$V, $f_{mod} = 1$ kHz, $p = 9 \pm 1$ mbar. The numbers beside the distribution width ratio refers to the calibration method used: (1) calibrated with distributions, (2) calibrated with PSDs

The Data Set	$\kappa_{y,high}/\kappa_{y,low}$	$\sigma_{y,high}/\sigma_{y,low}$ 1	$\sigma_{y,high}/\sigma_{y,low}$ 2
A	1.858 ± 0.020	0.580 ± 0.002	0.732 ± 0.003
B	1.665 ± 0.004	0.731 ± 0.001	0.771 ± 0.001
C	1.879 ± 0.004	0.734 ± 0.001	0.727 ± 0.002
D	1.184 ± 0.002	0.936 ± 0.002	0.922 ± 0.002

Table 2: The ratios of the stiffnesses and position widths at the different beam intensities in the vertical direction. Data sets: (**A**) $A_{mod} = 5$V, $f_{mod} = 1$ kHz, $p = 30 \pm 1$ mbar (**B**) $A_{mod} = 5$V, $f_{mod} = 1$ kHz, $p = 20 \pm 1$ mbar, (**C**) $A_{mod} = 5$V, $f_{mod} = 1$ kHz, $p = 10 \pm 1$ mbar, (**D**) $A_{mod} = 5$V, $f_{mod} = 1$ kHz, $p = 9 \pm 1$ mbar. The numbers beside the distribution width ratio refers to the calibration method used: (1) calibrated with distributions, (2) calibrated with PSDs

It can be seen from the distributions that using the different methods we find that the amplitudes of oscillation are not in line, despite both methods being theoretically justified. The widths of the distributions and the amplitude of oscillation in the underdamped regime using position distributions to calibrate the data are approximately 3 times those found using the PSDs. Both methods yield reasonable results in which it can be seen that the particle oscillates within the limits of the beam width. Either calibration result considered are limited by approximations, such that the temperature in the vacuum chamber was not measured at the given pressures, but it was assumed that it was fixed at room temperature. Using the expected position distribution to calibrate the data, we are limited by the approximations made to arrive at a perfectly harmonic potential where damping and scattering effects are not taken into account. On the other hand, using the PSDs to calibrate the signals, although the damping rate is considered in the fitting, the calibration constant itself is not dependent on the damping, and background noise in the PSD are not considered. Looking at the ratios as noted in tables 1 and 2, we can see that the methods are consistent in the lower pressures (≤ 20 mbar) where the particle oscillates in the underdamped regime. Deviation between the ratios are highest when the particle is oscillating in the critical damping regime at pressure 30 mbar, this is to be expected, as damping effects are not taken into consideration when formulating the trap's potential (eq. 2.13), thus the particle's distribution becomes independent of the high damping contrary to what is expected in such regime.

4.3.1 Time evolution of the distributions

In order to study the transition of the nanosphere from a state where the beam intensity is low to a state where it is higher, we find the width of the distributions in time, the code applied to preform this is in appendix D. In this analysis, we focus on beam modulations with an amplitude of 5 V, as the ratio between the widths is higher, thus a transition is expected to be observed more clearly. The following figures (4.13, 4.14 and 4.15) are found with the data calibrated using position distributions, either calibration methods would yield the same trends since the calibrations are taken to be linear. The time at which the modulation is applied as well as the theoretical relaxation time (eq. 2.22) are depicted on the figures.

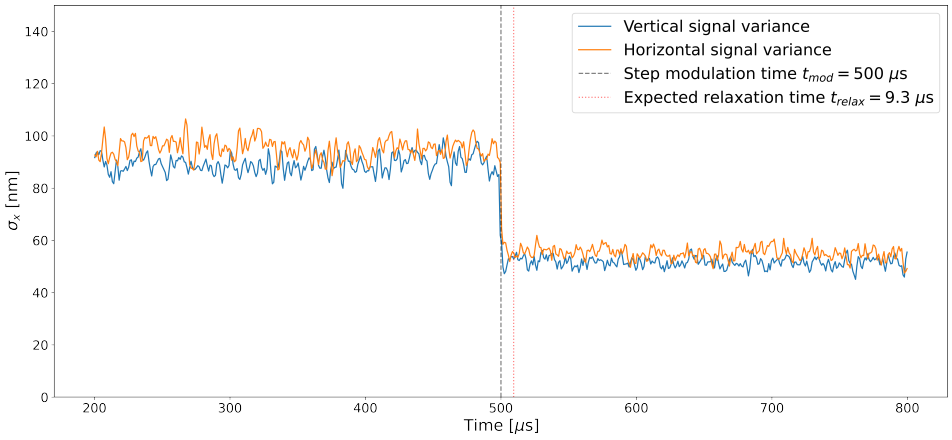

Figure 4.13: The evolution of the particle's position distribution's width σ with the application of step modulation at 30 ± 1 mbar

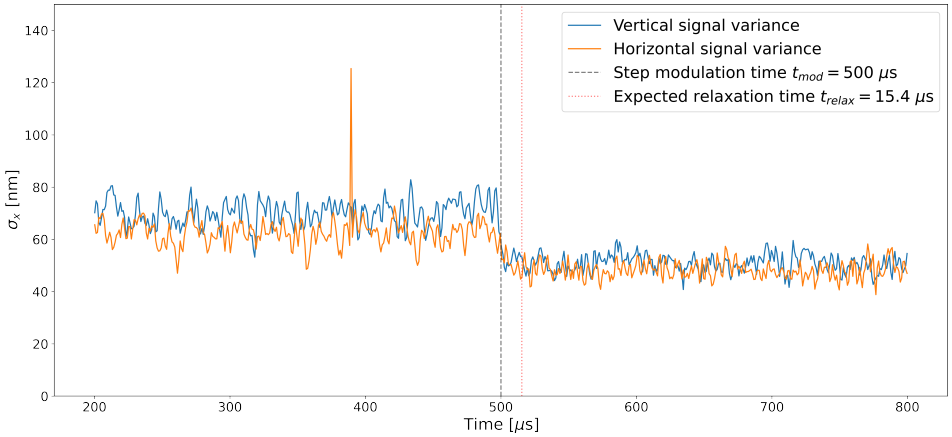

Figure 4.14: The evolution of the particle's position distribution's width σ with the application of step modulation at 20 ± 1 mbar

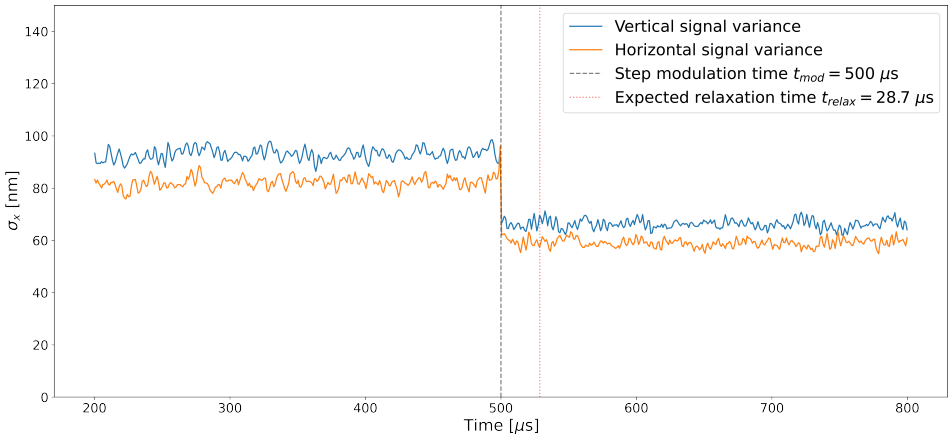

Figure 4.15: The evolution of the particle's position distribution's width σ with the application of step modulation at 10 ± 1 mbar

Prior to discussing the results, it should be noted that due to the limited statistical data in the second set, at 20 mbar, the fluctuations in the the distribution width are high. Looking at the data set taken at a pressure of 30 mbar (fig. 4.13), we see that the transition from the initial state with a lower beam intensity to a final state with higher beam intensity is instantaneous. From fitting the PSDs at this pressure, we found that the particle oscillates in the critical damping regime, which goes beyond the theoretical discussion of the research. However, as we transition to the underdamped regime (fig. 4.15), where we expect that the particle takes time to transition from the initial state to the final, we still find that the transition is instantaneous.

The conflict in results and theory is expected to be a result of either, first, the limitation of the theoretical basis on the dynamics of optical trapping in the underdamped regime, or second , on the limitations of the setup itself and the data acquisition methods.

5 Conclusions

Upon trapping the silica nanosphere in the optical tweezer and modulating its intensity via a generated square wave with different amplitudes, the vacuum chamber's valve is opened allowing for the damping rate to decrease. As the air is being emptied from the chamber, data sets were collected at different pressures. Via this process, we observed that the particle's oscillation frequency increases with increasing the beam intensity, this occurs in both the critically damped and the underdamped regimes. After fitting the PSDs we calibrate the signals in volts to find the displacement of the particle in the trap in nanometers. Two calibration methods are applied and compared, although both methods are reasonable considering the trends which follow from them align with theoretical expectations, the methods disagree regarding the amplitude of oscillation. An experimental calibration at different laser beam intensities could be preformed in the future to be able to get a better picture on how confined the particle is, and arrive at better numerical analysis on how tightly the nanosphere oscillates.

With the calibrated data we find that the position distribution widths increase with increasing the intensity of the trapping beam. Focusing on the results at the underdamped regime, we find that when the beam stiffness is increased by approximately 18%, achieved by modulating the beam with a square wave function of amplitude 0.5 V, the distribution width decreases by approximately 6%. When the increase in stiffness is approximately 88%, achieved by a modulation with amplitude 5 V, the distribution width decreases by approximately 30%. We further explore the dynamics of the particle by looking at how the distribution width evolves with time, allowing us to observe how the trapped particle transitions from a state where the beam intensity is low to a state where the beam intensity is high. We found that the transition between the two states is instantaneous contrary to theory, such that we expected that the transition would take some time given by a relaxation time of approximately 28 μs. The difference between the expectations and data analysis is underlined in either the limitations of the setup, or in limitations in the theoretical basis, leaving us with an open question: Do levitated nanospheres in an optical trap which changes suddenly in intensity in the underdamped regime transition between two states instantaneously?

This question would potentially be answered by further investigating the theoretical basis of the dynamics of levitated particles in the underdamped regime, as the phenomena behind it has not been yet fully established and realised. Improvements in the setup that would allow us to achieve higher levels of vacuum will also allow us to better understand and back the theory.

6 Acknowledgements

With the completion of my Bachelor research project, I would like to express my gratitude to those who helped me achieve this. First I would like thank my supervisor Steven Hoekstra for taking me in to the research group, and for guiding me throughout the process. I would also like to thank Mina Morshed, the PhD candidate in the group, for allowing me to ambush her with my questions and concerns and for getting me acquainted with the experiment along with Carlos Alarcon, the Masters student in the group.

References

[1] Arthur Ashkin. "Beginnings". In: *Optical Trapping And Manipulation Of Neutral Particles Using Lasers: A Reprint Volume With Commentaries*. World Scientific Publishing Company, 2006, pp. 3–19. ISBN: 9789810240578.

[2] *Clausius-Mossotti equation*. DOI: 10.1093/oi/authority.20110803095616156. URL: https://www.oxfordreference.com/view/10.1093/oi/authority.20110803095616156.

[3] Jan Gieseler. "Dynamics of optically levitated nanoparticles in high vacuum". In: *GRIN Publishing Munich, Germany* (2014). Phd Thesis.

[4] Jan Gieseler and James Millen. "Levitated Nanoparticles for Microscopic Thermodynamics-A Review". In: *Entropy (Basel)* 20 (5 2018). DOI: 10.3390/e20050326.

[5] Yasuhiro Harada and Toshimitsu Asakura. "Radiation forces on a dielectric sphere in the Rayleigh scattering regime". In: *Optics Communications* 124 (5-6 1996), pp. 529–541. ISSN: 0030-4018. DOI: 10.1016/0030-4018(95)00753-9.

[6] Coherent inc. *Mephisto MOPA*. URL: https://www.coherent.com/lasers/cw-solid-state/mephisto.

[7] Ignacio A. Martínez et al. "Engineered swift equilibration of a Brownian particle". In: *Nature Physics* 12 (9 2016), pp. 843–846. DOI: 10.1038/nphys3758.

[8] James Millen and Jan Gieseler. "Single Particle Thermodynamics with Levitated Nanoparticles". In: *Thermodynamics in the Quantum Regime: Fundamental Aspects and New Directions*. Ed. by Felix Binder et al. Cham: Springer International Publishing, 2018, pp. 853–885. ISBN: 978-3-319-99046-0. DOI: 10.1007/978-3-319-99046-0_35.

[9] Lukas Novotny and Bert Hecht. "Propagation and focusing of optical fields". In: *Principles of Nano-Optics*. 2nd ed. Cambridge University Press, 2012, pp. 45–85. DOI: 10.1017/CBO9780511794193.005.

[10] Giuseppe Pesce et al. "Optical tweezers: theory and practice". In: *The European Physical Journal Plus* 135 (12 2020). DOI: 10.1140/epjp/s13360-020-00843-5.

[11] Paolo Polimeno et al. "Optical tweezers and their applications". In: *Journal of Quantitative Spectroscopy and Radiative Transfer* 218 (2018), pp. 131–150. ISSN: 0022-4073. DOI: https://doi.org/10.1016/j.jqsrt.2018.07.013.

[12] Zwanzig Robert. "Brownian Motion and Langevin Equations". In: *Nonequilibrium Statistical Mechanics*. Oxford University Press, 2001, pp. 3–24. ISBN: 9780195140187.

[13] Jamie Vovrosh. "Parametric feedback cooling and squeezing of optically levitated particles". In: *University of Southampton* (2018). Phd Thesis.

A Code - data separation, low frequency analysis and PSDs

After uploading the data file as csv and separating the columns for the time, vertical and horizontal signal channels, the lists are run through the following functions

```
import csv
import numpy as np
import matplotlib.pyplot as plt
import pandas as pd
import scipy as sp
import os
import scipy.stats as stats
from scipy.stats import norm
import matplotlib.mlab as mlab
from statistics import mean
# # # # # # # # # # # # # # # # # # # # # # # # # # # # # # # # # # #

#high and low stiffness separation:

#make lists for new values:
#vhs, vls, hhs, hls, hji, lji
#(v: vertical signal, h:horizontal signal)
#(hs: high stiffness, ls: low stiffness)

#data input:
#the raw data lists (t: time, ver: vertical channel,
#hor: horizontal channel, mod: modulation channel)

#the function:
def high_and_low(t, ver, hor, mod, thres, vhs, vls, hhs, hls, ths, tls, hji, lji):
    #getting the indices of high stiffness:
    stl = -1
    xl = []
    low_index = []
    for i in mod:
        if i < thres:
            try:
                xl = mod.index(i, stl+1)
            except ValueError:
                break
            else:
                low_index.append(xl)
                stl = xl

    #getting the indices of low stiffness:
    sth = -1
    xh = []
    high_index = []
    for i in mod:
        if i > thres:
            try:
                xh = mod.index(i, sth+1)
            except ValueError:
                break
```

```
            else:
                high_index.append(xh)
                sth = xh

    #define signal lists before cuts:
    vhs1 = []
    vls1 = []
    hhs1 = []
    hls1 = []
    ths1 = []
    tls1 = []

    #Adding values to time and signal lists:
    for i in high_index:
        vhs1.append(ver[i])
        hhs1.append(hor[i])
        ths1.append(t[i])

    for i in low_index:
        vls1.append(ver[i])
        hls1.append(hor[i])
        tls1.append(t[i])

    #making sure cut data has full jumps:
    #high:
    for i in range(len(ths1)):
        x = ths1[i]
        y = ths1[i-1]
        if x - y > 4.5 * 10**(-6):
            hji.append(i)
    #low:
    for i in range(len(tls1)):
        x = tls1[i]
        y = tls1[i-1]
        if x - y > 4.5 * 10**(-6):
            lji.append(i)

    #cutting data:
    for i in ths1[hji[0]:hji[-1]]:
        ths.append(i)
    for i in vhs1[hji[0]:hji[-1]]:
        vhs.append(i)
    for i in hhs1[hji[0]:hji[-1]]:
        hhs.append(i)
    for i in tls1[lji[0]:lji[-1]]:
        tls.append(i)
    for i in vls1[lji[0]:lji[-1]]:
        vls.append(i)
    for i in hls1[lji[0]:lji[-1]]:
        hls.append(i)

# # # # # # # # # # # # # # # # # # # # # # # # # # # # # # # # # # #
```

```
#reject low frequencies/ oscillations

#make lists for new values:
#(1)vhs_norm, (2)vls_norm, (3)hhs_norm, (4)hls_norm
#these will have the values of the oscillations around the zero point

#not using butter because that gets rid of quite a lot of the signal
#this takes the average of a jump (where the modulation occured) and subtracts the mean

#data input:
#vhs, vls, hhs, hls, hji, lji

#the function:
def low_freq_filter(vhs, vls, hhs, hls, hji, lji, vhs_norm, vls_norm, hhs_norm, hls_norm):
    vhs_norm1 = []
    vhs_norm1_lst = []
    vls_norm1 = []
    vls_norm1_lst = []
    hhs_norm1 = []
    hhs_norm1_lst = []
    hls_norm1 = []
    hls_norm1_lst = []

    #vhs
    for i in range(0,len(hji[:-2])):
        x = vhs[hji[i]:hji[i+1]]
        vhs_norm1.append(np.subtract(vhs[hji[i]:hji[i+1]], mean(x)))

    for i in vhs_norm1:
        vhs_norm1_lst.append(i.tolist())

    for i in vhs_norm1_lst:
        for j in i:
            vhs_norm.append(j)

    #vls
    for i in range(0,len(lji[:-2])):
        x = vls[lji[i]:lji[i+1]]
        vls_norm1.append(np.subtract(vls[lji[i]:lji[i+1]], mean(x)))

    for i in vls_norm1:
        vls_norm1_lst.append(i.tolist())

    for i in vls_norm1_lst:
        for j in i:
            vls_norm.append(j)

    #hhs
    for i in range(0,len(hji[:-2])):
        x = hhs[hji[i]:hji[i+1]]
        hhs_norm1.append(np.subtract(hhs[hji[i]:hji[i+1]], mean(x)))

    for i in hhs_norm1:
```

```
        hhs_norm1_lst.append(i.tolist())

    for i in hhs_norm1_lst:
        for j in i:
            hhs_norm.append(j)

    #hls
    for i in range(0,len(lji[:-2])):
        x = hls[lji[i]:lji[i+1]]
        hls_norm1.append(np.subtract(hls[lji[i]:lji[i+1]], mean(x)))

    for i in hls_norm1:
        hls_norm1_lst.append(i.tolist())

    for i in hls_norm1_lst:
        for j in i:
            hls_norm.append(j)

# # # # # # # # # # # # # # # # # # # # # # # # # # # # # # # # # # #

#FFT function
#inputs: vhs_norm, vls_norm, hhs_norm, hls_norm + f_s sampling rate

#need to define empty lists for PSD data: (1) psd_vhs, (2) psd_vls, (3) psd_hhs, (4) psd_hls

def FFTviaPSD(vhs_norm, vls_norm, hhs_norm, hls_norm, psd_vhs, psd_vls, psd_hhs, psd_hls,
f_s, figname):
    plt.figure(figsize=(15,7))

    vtot = []
    htot = []

    for i in vhs_norm:
        vtot.append(i)
    for i in vls_norm:
        vtot.append(i)

    for i in hhs_norm:
        htot.append(i)
    for i in hls_norm:
        htot.append(i)

    vh_psd_plt = plt.psd(vhs_norm, Fs=f_s, label='vertical - high stiffness')
    vl_psd_plt = plt.psd(vls_norm, Fs=f_s, label='vertical - low stiffness')
    v_psd_plt = plt.psd(vtot, Fs=f_s, color='black', alpha=0.5)

    hh_psd_plt = plt.psd(hhs_norm, Fs=f_s, label='horizontal - high stiffness')
    hl_psd_plt = plt.psd(hls_norm, Fs=f_s, label='horizontal - low stiffness')
    h_psd_plt = plt.psd(htot, Fs=f_s, color='black', alpha=0.5, label='totals')

    plt.legend()
    plt.show()
```

```
    for i in vh_psd_plt:
        psd_vhs.append(vh_psd_plt)

    for i in vl_psd_plt:
        psd_vls.append(vl_psd_plt)

    for i in hh_psd_plt:
        psd_hhs.append(hh_psd_plt)

    for i in hl_psd_plt:
        psd_hls.append(hl_psd_plt)

# # # # # # # # # # # # # # # # # # # # # # # # # # # # # # # # # # #

#getting the frequencies from the PSD:

def frequencies(psd_vhs, psd_vls, psd_hhs, psd_hls, vhP, vhf, vlP, vlf, hhP, hhf, hlP, hlf):
    #first get list of power and frequency values,
    #reject the first two points where it peaks at frequency=0
    vh_psd_P = psd_vhs[1][0].tolist()
    vh_psd_f = psd_vhs[1][1].tolist()
    vl_psd_P = psd_vls[1][0].tolist()
    vl_psd_f = psd_vls[1][1].tolist()

    hh_psd_P = psd_hhs[1][0].tolist()
    hh_psd_f = psd_hhs[1][1].tolist()
    hl_psd_P = psd_hls[1][0].tolist()
    hl_psd_f = psd_hls[1][1].tolist()

    for i in vh_psd_P:
        vhP.append(i)
    for i in vh_psd_f:
        vhf.append(i)
    for i in vl_psd_P:
        vlP.append(i)
    for i in vl_psd_f:
        vlf.append(i)
    for i in hh_psd_P:
        hhP.append(i)
    for i in hh_psd_f:
        hhf.append(i)
    for i in hl_psd_P:
        hlP.append(i)
    for i in hl_psd_f:
        hlf.append(i)

# # # # # # # # # # # # # # # # # # # # # # # # # # # # # # # # # # #
```

B Code - calibration via distributions

This code follows after separating the data points at high and low stiffness, filtering the low frequencies and defining lists for the PSD data points.

```
#finding the variables (frequency and stiffness)

#frequency:
def f0(f_list, P_list):
    return f_list[P_list.index(max(P_list))]

#for calibration:
import math
from scipy.constants import pi, k, N_A

r = 71.5 * 10**(-9) #particle radius in m
T = 293 #room temperature
den = 1850 #density of silica in kg/m taken from the website that sells the particles
vol = (3/4) * pi * r**3 #volume of the particle
mass = den * vol

#stiffness:
def stfns(f0):
    return (2*pi*f0)**2 * mass

#the calibration constant
#sigma is the sqrt of the variance found from fitting the distributions
def calb(sigma, stfns):
    return (1/sigma) * math.sqrt(k * T /stfns)

#calibrating the data:
#V_list: the list of signal in V data (after frequency filtering)
def cal_list(calb, V_list):
    return [calb * i for i in V_list]
```

C Code - calibration via PSD fitting

This code follows after separating the data points at high and low stiffness, filtering the low frequencies and defining lists for the PSD data points.

```
#defining the constants;
import math
from scipy.constants import pi, k, N_A, epsilon_0, c

r = 71.5 * 10**(-9) #particle radius in m
T = 293 #temperature

den = 1850 #density of silica in kg/m
vol = (4/3) * pi * r**3 #volume of the particle
mass = den * vol #particle mass

d_m=0.372*1e-9 #diameter of air molecules
M = 28.97 * 10**(-3) #air in 1 mol in kg/mol
mu_v=2*np.sqrt(M*k*T/N_A)/(3*np.sqrt(pi)*pi*d_m**2) #viscocity coeffecient

# # # # # # # # # # # # # # # # # # # # # # # # # # # # # # # # #

#damping rate - defines expected damping rate:
def gamma(pres, temp):
    meanfreepath = k*temp/(math.sqrt(2)*pi*(d_m)**2 * pres)
    K_n = meanfreepath/r  #Knudsen number
    C_k = 0.3 * K_n /(0.785 + 1.152 * K_n + K_n**2);
    return (6*pi*mu_v*r /mass) * (0.619/(0.619 + K_n)) * (1+C_k)

#the equation to be fitted (eq. 3.7)
def theoreticalfit(fre, damp,f0,A):
    return [((k*T/(pi*mass))* 2*pi*damp/(((2*pi*f0)**2 - (2*pi*i)**2)**2 +
        (2*pi*i)**2 * (2*pi*damp)**2)) * A**2 for i in fre]

#the calibration constant in m/V:
def calib(A):
    return 1/A

# # # # # # # # # # # # # # # # # # # # # # # # # # # # # # # # #
#lmfit module has to be installed
from lmfit import Model, Parameter, report_fit

model = Model(theoreticalfit, independent_vars=['fre'])

results = model.fit(vhPA[5:], fre=vhfA[5:], damp=100000, f0=100000, A=1e6)

print(lmfit.fit_report(results.params)) #outputs the fitted parameters and their errors
```

D Code - time evolutions

The code in this section is used to compile data over one period of modulation to get the time evolution of the distribution widths. This follows after applying the code in appendix A and calibrating the signal

```
#separating the data during half periods for each of the orientations:
hh_list = []
for i in range(len(ljiA)):
    hh_list.append(hh_calA[ljiA[i-1]:ljiA[i]])

hl_list = []
for i in range(len(ljiA[:-1])):
    hl_list.append(hl_calA[ljiA[i-1]:ljiA[i]])

vh_list = []
for i in range(len(ljiA)):
    vh_list.append(vh_calA[ljiA[i-1]:ljiA[i]])

vl_list = []
for i in range(len(ljiA[:-1])):
    vl_list.append(vl_calA[ljiA[i-1]:ljiA[i]])

#The lists are transposed
hl_listT = pd.DataFrame(hl_list).T.values.tolist()

hh_listT = pd.DataFrame(hh_list).T.values.tolist()

vl_listT = pd.DataFrame(vl_list).T.values.tolist()

vh_listT = pd.DataFrame(vh_list).T.values.tolist()

#Time over one period, for modulation frequency 1kHz:
t=np.linspace(0, 10000, num=10000)

#finding the distribution widths:
sigmas_vh=[]
sigmas_vl=[]
for i in vh_listT:
    _, sigs = sp.stats.norm.fit(i)
    sigmas_vh.append(sigs)

for i in vl_listT:
    _, sigs = sp.stats.norm.fit(i)
    sigmas_vl.append(sigs)

sigmas_hh=[]
sigmas_hl=[]
for i in hh_listT:
    _, sigs = sp.stats.norm.fit(i)
    sigmas_hh.append(sigs)

for i in hl_listT:
    _, sigs = sp.stats.norm.fit(i)
    sigmas_hl.append(sigs)
```

```
#the plot:
plt.figure(figsize=(20,9))
plt.plot(t_proper, (sigmas_vl+sigmas_vh), label='Vertical signal variance')
plt.plot(t_proper, (sigmas_hl+sigmas_hh), label='Horizontal signal variance')
plt.plot([5000,5000],[0,400], '--', color='black', alpha=0.5, label='Step modulation time')
plt.plot([5026,5026],[0,400], ':', color='red', alpha=0.5, label='Expected relaxation time')

plt.legend(fontsize=20)


plt.ylabel('$\sigma_x$ [nm]', fontsize=20)
plt.xlabel('Time [nm]', fontsize=20)

plt.yticks(fontsize=16)
plt.xticks(fontsize=16)

plt.ylim([0,150])
```